

Validation of an asymptotic zone conditional expression for turbulent burning velocity against DNS database

By K. Y. Huh[†], S. H. Kim and S. Kim[†]

Zone conditional formulations for the Reynolds averaged reaction progress variable are used to derive an asymptotic expression for turbulent burning velocity. New DNS runs are performed for validation in a statistically one dimensional steady state configuration. A parametric study is performed with respect to turbulent intensity, integral length scale, density ratio and laminar flame speed. Results show good agreement between DNS results and the asymptotic expression in terms of measured maximum flame surface density and estimated turbulent diffusivity in unburned gas.

1. Motivation and objectives

There has been controversy about the definition of turbulent burning velocity, which is the mean propagation speed of a flame brush in turbulent premixed combustion. Although it is a quantity of engineering significance in many combustion devices, experimental correlations have shown much scatter in different flame configurations and test conditions. There are some theoretical or analytical expressions with arbitrary tuning constants (Peters 1999), which have similar functional forms with experimental correlations (Abdel-Gayed *et al.* 1987). The current consensus is that there is yet no predictive formula reliable in a wide range of combustion situations. A pessimistic view is that there may be no unique measurable quantity to be defined as the turbulent burning velocity in any given experimental condition (Driscoll 2003). However confusion may come from the fact that we have not considered a complete list of relevant parameters or physical phenomena to characterize a turbulent premixed flame, e. g., external pressure gradient imposed in stagnating (Liu & Lenze 1988) or buoyant flow (Khokhlov *et al.* 1996) or flame instability to increase flame surface density at a higher ambient pressure (Kobayashi *et al.* 1996).

Some form of averaging is essential to handle randomly fluctuating scalars and reaction rates in turbulent combustion. Conditional averaging has proved useful to reduce such fluctuation, while unconditional Favre averaging does not allow a logical approach for closure of the nonlinear mean reaction rate. The conditional moment closure model (Klimenko & Bilger 1999) which involves conditional averaging with respect to mixture fraction has been successful in turbulent nonpremixed combustion problems (Kim & Huh 2004). Choice of the conditioning variable may be arbitrary as long as it contributes to significant reduction of fluctuation from any conditional mean value. Zone conditional averaging is a reasonable choice for turbulent premixed combustion at a high Damkohler number. It is because much of the fluctuation originates from transition between burned and unburned regions in addition to generic turbulent fluctuation in each region. In

[†] Mechanical Eng. Dept. Pohang University of Science and Technology, Korea

previous work the zone conditionally averaged mass and momentum equations were derived with the closure assumptions for unknown surface average quantities (Lee & Huh 2004; Lee *et al.* 2004). Validation was performed against the DNS database of a steady flame brush (Nishiki *et al.* 2002), although at relatively low turbulence Reynolds and Damkohler numbers. In this study new DNS runs are made to validate the predictive formula for turbulent burning velocity with parametric study to evaluate independently the effects of turbulent intensity, integral length scale, density ratio and laminar flame speed.

2. Mathematical Formulation

2.1. Definition of zone conditional averaging

We introduce the Heaviside function defined as

$$H_{c^*}(\mathbf{x}, t, c) = H(c - c^*) = \begin{cases} 1 & \text{if } c(\mathbf{x}, t) \geq c^* \\ 0 & \text{otherwise} \end{cases} \quad (2.1)$$

where c^* is set equal to 0.5. The idea is to separate the instantaneous reaction field into three distinct zones; unburned ($\rho = \rho_u$), burned ($\rho = \rho_b$) and thin reaction zone ($\rho_b < \rho < \rho_u$). The iso- c surface defines the flame surface which separates the zone of $c(\mathbf{x}, t) \geq c^*$ from the zone of $c(\mathbf{x}, t) \leq c^*$. In the limit of a high Damkohler number the reaction zone thickness is less than any turbulence length scale and the probability of $0 < c < 1$ becomes negligibly small. Then the expectation of H_{c^*} is equal to Reynolds averaged reaction progress variable as

$$\langle H_{c^*} \rangle = \bar{c}. \quad (2.2)$$

The overbar and $\langle \cdot \rangle$ notation with no subscript represent an unconditional ensemble average and may be used interchangeably. For any quantity, Φ , it holds that

$$\langle H_{c^*} \Phi \rangle = \bar{c} \langle \Phi \rangle_b \quad (2.3)$$

$$\langle (1 - H_{c^*}) \Phi \rangle = (1 - \bar{c}) \langle \Phi \rangle_u \quad (2.4)$$

where $\langle \Phi \rangle_b$ and $\langle \Phi \rangle_u$ are the conditional averages in burned and unburned region respectively. Define that

$$\Phi_i = \langle \Phi \rangle_i + \Phi'_i \quad (2.5)$$

where the subscript i can be any of u , b , su or sb . The notations, sb and su , represent the conditional quantities in burned and unburned gas adjacent to the thin reaction zone as shown in Fig. 1. The prime notation may represent an unconditional or a conditional fluctuation according to the definition of the average. The two averages, $\langle \Phi \rangle_u$ and $\langle \Phi \rangle_{su}$ (or $\langle \Phi \rangle_b$ and $\langle \Phi \rangle_{sb}$), are not in general equal to each other. When integrated over volume, the former represents a volumetric average in unburned (or burned) gas while the latter represents a surface average on the unburned (or burned) side of a flame surface. Conditional density fluctuation is ignored as negligible with constant ρ_b and ρ_u . Since variable density and chemical reaction are confined to the thin reaction zone, all reaction terms can be represented as simple interfacial transfer in terms of the surface average quantities, su or sb , on either side of a flame surface.

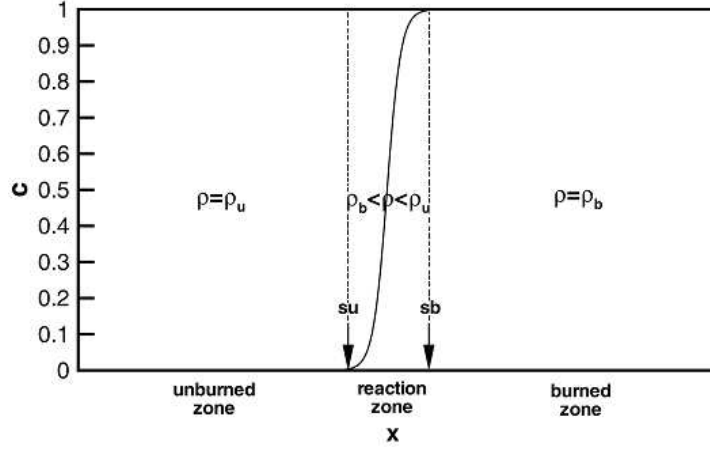


FIGURE 1. Illustration of instantaneous reaction field around a flamelet surface.

2.2. Derivation of \bar{c} transport equation

The instantaneous local balance equation for reaction progress variable is written as,

$$\frac{\partial c}{\partial t} + \mathbf{v} \cdot \nabla c = S_d |\nabla c| \quad (2.6)$$

where the reaction progress variable, c , is defined as,

$$c = \frac{T - T_u}{T_b - T_u} \quad \text{or} \quad c = \frac{Y_F - Y_F^u}{Y_F^b - Y_F^u}. \quad (2.7)$$

T , T_u and T_b are respectively local, unburned and burned gas temperatures. Y_F , Y_F^u and Y_F^b are the fuel mass fractions of local, unburned and burned gas. The two definitions in Eq. (2.7) are equivalent for a unity Lewis number with no heat loss and compressibility effects. Temporal and spatial derivatives of the Heaviside function are given as,

$$\frac{\partial H(c - c^*)}{\partial t} = \delta(c - c^*) \frac{\partial c}{\partial t} \quad (2.8)$$

$$\nabla H(c - c^*) = \delta(c - c^*) \nabla c. \quad (2.9)$$

A balance equation for the Heaviside function, H_{c^*} , can be derived from Eqs. (2.6), (2.8) and (2.9) as,

$$\frac{\partial H_{c^*}}{\partial t} + \mathbf{v} \cdot \nabla H_{c^*} = S_L \Sigma \quad (2.10)$$

where S_d is assumed to be equal to the laminar flame speed S_L . The instantaneous flame surface density Σ is defined as,

$$\Sigma = |\nabla c| \delta(c - c^*) \quad (2.11)$$

Taking an ensemble average of Eq. (2.10) we have a transport equation for the Reynolds averaged reaction progress variable as,

$$\frac{\partial \bar{c}}{\partial t} + \langle \mathbf{v} \rangle_{su} \cdot \nabla \bar{c} = \langle \mathbf{v}'_{su} \cdot \mathbf{n}' \rangle_s \Sigma_f + S_L \Sigma_f \quad (2.12)$$

where the flame surface density, Σ_f , is an ensemble average of Σ . In Eq. (2.12), the surface average of Φ , $\langle \Phi \rangle_s$, is defined as $\langle \Phi \rangle_s = \langle \Phi \Sigma \rangle / \Sigma_f$, which is different from

the unconditional BML formulation. The surface averages here are taken to be on the unburned side for modelling and interpretation in the following. It is, however, equally valid to write Eq. (2.12) in terms of the surface averages on the burned side for an infinitesimally thin flamelet. \mathbf{n} is a unit normal vector on a flame surface toward the unburned side given as,

$$\mathbf{n}(\mathbf{x}, t) = -(\nabla c / |\nabla c|)_{c=c^*}. \quad (2.13)$$

Note that $\nabla H_{c^*} = -\mathbf{n}\Sigma$. The laminar flame speed, S_{Lu} , is the displacement speed relative to adjacent unburned gas, i.e. $\mathbf{v}_s = \mathbf{v}_{su} + \mathbf{n}S_{Lu}$, where \mathbf{v}_s is the velocity of the iso- c flame surface. In case counter-gradient diffusion is dominant over gradient transport with a large heat release parameter and weak turbulence, the flame surface density, Σ_f , may be modelled simply as,

$$\Sigma_f = 4\Sigma_{max}\bar{c}(1 - \bar{c}) \quad (2.14)$$

where Σ_{max} is the maximum at $\bar{c} = 0.5$. This parabolic profile is shown to be accurate in many experiments (Deschamps *et al.* 1992), while the peak \bar{c} tends to increase with increasing gradient diffusion (Lee *et al.* 2000).

2.3. Asymptotic expression for turbulent burning velocity

The transport equation, Eq. (2.12), for the Reynolds averaged reaction progress variable can be rewritten as,

$$\frac{\partial \bar{c}}{\partial t} + \langle \mathbf{v} \rangle_u \cdot \nabla \bar{c} = (\langle \mathbf{v} \rangle_u - \langle \mathbf{v} \rangle_{su}) \cdot \nabla \bar{c} + \langle \mathbf{v}'_{su} \cdot \mathbf{n}' \rangle_s \Sigma_f + S_{Lu} \Sigma_f. \quad (2.15)$$

The first term on the RHS of Eq. (2.15) is modelled as,b

$$(\langle \mathbf{v} \rangle_u - \langle \mathbf{v} \rangle_{su}) \cdot \nabla \bar{c} = f(u' / S_{Lu}^0, Ka) D_{tu} \nabla^2 \bar{c} \quad (2.16)$$

where D_{tu} is turbulent diffusivity in unburned gas and the function, f , represents the effect of nonpassive nature of a flame surface in terms of the ratio, u' / S_{Lu}^0 , and the Karlovitz number. The difference between the surface and volume average velocities comes from diffusive turbulent eddy motions in unburned gas without any externally imposed pressure gradient. The second term on the RHS of Eq. (2.15) is modelled as (Lee & Huh 2004),

$$\langle \mathbf{v}'_{su} \cdot \mathbf{n}' \rangle_s \Sigma_f = K \langle k \rangle_u^{0.5} \langle \mathbf{n}' \cdot \mathbf{n}' \rangle^{0.5} \Sigma_f = K \langle k \rangle_u^{0.5} (1 - \langle \mathbf{n} \rangle_s \cdot \langle \mathbf{n} \rangle_s)^{0.5} \Sigma_f \quad (2.17)$$

where I_0 is the mean stretch factor for laminar flame speed. K is a dimensionless constant of order unity. The quantity, $\langle \mathbf{v}'_{su} \cdot \mathbf{n}' \rangle_s$, is shown to be positive and approximately constant through a flame brush in the DNS database (Nishiki *et al.* 2002). The transport equation for the Reynolds averaged reaction progress variable can now be written for a one-dimensional steady propagating flame as,

$$U_T \frac{d\bar{c}}{dx} = f(u' / S_{Lu}^0, Ka) D_{tu} \frac{d^2 \bar{c}}{dx^2} + K \langle k \rangle_u^{0.5} (1 - \langle \mathbf{n} \rangle_s \cdot \langle \mathbf{n} \rangle_s)^{0.5} \Sigma_f + I_0 S_{Lu}^0 \Sigma_f \quad (2.18)$$

where the turbulent flame speed, U_T , may be obtained asymptotically by assuming exponential decay of \bar{c} as \bar{c} approaches zero.

$$\frac{d\bar{c}}{dx} = a_1 \bar{c} \quad \text{as } \bar{c} \rightarrow 0 \quad (2.19)$$

The following relationships should hold asymptotically at the leading edge.

$$\frac{d^2\bar{c}}{dx^2} = a_1^2\bar{c}, \quad \langle n_x \rangle_s = 1, \quad \Sigma_f = \frac{d\bar{c}}{dx} = a_1\bar{c} \quad \text{as } \bar{c} \rightarrow 0 \quad (2.20)$$

The magnitude of the mean unit normal vector, $\langle n_x \rangle_s$, should approach unity as $\bar{c} \rightarrow 0$ or $\bar{c} \rightarrow 1$, as burned or unburned gas may exist only on one side of a plane normal to the propagation direction. The constant a_1 is determined as $4\Sigma_{max}$ according to Eqs. (2.14) and (2.20). Then, an asymptotic formula for U_T is given from Eq. (2.18) as,

$$U_T = 4f(u'/S_{Lu}^0, Ka)\Sigma_{max}D_{tu} + I_0S_{Lu}^0. \quad (2.21)$$

Note that the modeled term in Eq. (2.17) does not affect the asymptotic expression for turbulent burning velocity. In the following the function, f , and the mean stretch factor, I_0 , are assumed to be equal to unity for comparison with DNS results. Further investigation is required on these two parameters, while validity of this investigation will not be impaired considering uncertainties in the other estimated quantities, Σ_{max} and D_{tu} .

3. Methodology in DNS

Direct numerical simulation is performed to construct a new database for validation of Eq. (2.21) for turbulent burning velocity. Fully compressible Navier-Stokes equations with single step chemistry are solved:

$$\frac{\partial \rho}{\partial t} + \frac{\partial \rho u_i}{\partial x_i} = 0 \quad (3.1)$$

$$\frac{\partial \rho u_i}{\partial t} + \frac{\partial}{\partial x_j}(\rho u_i u_j) = -\frac{\partial p}{\partial x_i} + \frac{\partial \tau_{ij}}{\partial x_j} \quad (3.2)$$

$$\frac{\partial \rho e}{\partial t} + \frac{\partial}{\partial x_j}[(\rho e + p)u_j] = \frac{\partial u_j \tau_{ij}}{\partial x_i} + \frac{\partial}{\partial x_i}(\lambda \frac{\partial T}{\partial x_i}) + Q\omega \quad (3.3)$$

$$\frac{\partial \rho Y_R}{\partial t} + \frac{\partial}{\partial x_j}(\rho u_j Y_R) = \frac{\partial}{\partial x_i}(\rho D \frac{\partial Y_R}{\partial x_i}) - \omega \quad (3.4)$$

where

$$\rho e = \frac{1}{2}\rho u_i u_i + \frac{p}{\gamma - 1} \quad (3.5)$$

$$\tau_{ij} = \mu \left(\frac{\partial u_i}{\partial x_j} + \frac{\partial u_j}{\partial x_i} - \frac{2}{3}\delta_{ij} \frac{\partial u_k}{\partial x_k} \right) \quad (3.6)$$

$$\omega = A\rho Y_R \exp\left(-\frac{T_a}{T}\right) \quad (3.7)$$

p is the pressure, e is the internal energy and Q is the heat of reaction per unit mass of fresh mixture. A is a pre-exponential factor. T_a is the activation temperature. The gas mixture is assumed to be a perfect gas with a specific heat ratio of $\gamma=1.4$. Y_R is the mass fraction of reactant. The reaction progress variable is defined here as $c \equiv 1 - Y_R$. The thermal conductivity, λ , and the diffusion coefficient, D , are given as

$$\lambda = \mu c_p / Pr \quad \text{and} \quad D = \mu / (\rho Sc). \quad (3.8)$$

The viscosity, μ , is given as

$$\mu = \mu_u (T/T_u)^{0.76}. \quad (3.9)$$

Both the Prandtl number, Pr , and the Schmidt number, Sc , are set to be 0.7. These equations are integrated by a low storage fourth order Runge-Kutta method with a sixth order compact finite difference scheme for spatial discretization. Initial and inflow turbulence are homogeneous and isotropic. The DNS code is based on the finite difference method with inflow and outflow boundary conditions at the inlet and outlet. Periodic boundary conditions are assigned on the sides to represent an infinite planar flame. Nonreflective formulations are employed to avoid a nondissipative transient reflected from inlet or outlet boundary due to an arbitrary guess for the initial state. The number of mesh points is 178x128x128 in the flow direction and the other two normal directions, respectively. It was about the maximum number of mesh points that could be handled by a LINUX PC with 1 Gb RAM.

The simulation is performed from an initial condition for five eddy turnover times to reach a fully developed steady flame. Data are then sampled at a regular interval for a subsequent ten eddy turnover times for averaging and postprocessing. There are 64 sampled data sets during the period of ten eddy turnover times for each case. The inflow boundary condition is adjusted continuously to maintain the steady state and retain the flame brush in the computational domain.

4. Results and Discussion

The simulation conditions for the reference case are summarized in Table 1. The Damkohler number is 7.2, the turbulence Reynolds number is 116.4 and the Karlovitz number is 3.94. These estimations are based on thermal diffusivity, laminar flame speed, turbulent intensity and integral length scale given in the table. The Zeldovich number, Ze , is defined as T_a/T_b , where T_b is burned gas temperature. D_{th} is thermal diffusivity. l_c is chemical length scale given as D_{th}/S_{Lu}^0 , which corresponds to laminar flamelet thickness. Single step chemistry will not be a concern for the zone conditional formulations at a high Da , although the Da here is restricted by computational limitation. Figure 2 shows three dimensional images of a fluctuating flame brush for the reference case. There are about four or five computational cells assigned to resolve the internal structure of a laminar flamelet. The quasi steady flame brush is well confined in the domain throughout the sampling period. Flame surface momentarily forms a long finger protruding into burned gas, which either burns out to disappear or gets detached and convected downstream as an unburned pocket. Although not a serious concern, this may affect conditional statistics as the flame touches the outlet boundary.

Spatial variation of $\bar{\tau}$ and flame surface density in Figs. 3(a) and (b) show significant fluctuation due to stochastic behavior of a limited flame portion in the domain. The relationship between $\bar{\tau}$ and flame surface density is also stochastic to some extent in Fig. 3(c), but falls in the region bounded by a parabolic curve with the peak value of about 1.2. The mean values shown as hollow circles also form an approximate parabolic curve with the peak value of about 0.9 in Fig. 3(c). The instantaneous turbulent burning velocity is set equal to the inflow velocity corrected for minor movement of the flame brush at every time step. The mean turbulent burning velocity is 1.24 in Fig. 3(d) with fluctuation for the same reason as in Fig. 3(a) and (b). Here the turbulent burning velocity is estimated by Σ_{max} on the upper boundary curve, since the asymptotic gradient at the leading edge seems to correlate better with the upper curve than with the average curve

TABLE 1. Reference case

ρ_u/ρ_b	$S_{L_u}^0$	$u'/S_{L_u}^0$	u'	l_k	l_c	τ_t	τ_c	ν
4.0	0.314	2.38	0.7471	0.0229	0.0455	1.0424	0.1449	0.005
k	ϵ	ν_t	D_{th}	l_t	Ka	Re_t	Da	Ze
0.8373	0.4539	0.1390	0.0413	0.7788	3.94	116.4	7.2	4.0

in Fig. 3(c). There will be negligible fluctuation with no such ambiguity in experimental measurements or simulations in a much larger domain.

The volume and surface average velocities are shown at different times for the reference case in Fig. 4. Significant fluctuation of the conditional velocities is partly due to an insufficient number of samples for averaging on each cross sectional plane. While $\langle \mathbf{v} \rangle_b$ is greater than $\langle \mathbf{v} \rangle_u$ in most flame regions, crossover between $\langle \mathbf{v} \rangle_b$ and $\langle \mathbf{v} \rangle_u$ should occur near the leading edge for existence of a stabilized flame brush. The surface average velocities are close to the volume average velocities, while deviation occurs near the edges in Fig. 4. Deviation in unburned gas velocities occurs at the leading edge, while deviation in burned gas velocities occurs at the trailing edge. It is clear that the propagation characteristics depends on balance of momentum in the burned and unburned gas as well as transport of scalar quantities in a turbulent premixed flame.

A parametric study is performed for six cases in addition to the reference case with respect to turbulent intensity, integral length scale, density ratio and laminar flame speed as listed in Table 2. Three dimensional flame configurations are compared for all six test cases in Fig. 5. The flame shows more wrinkling with an increased flame surface density for the case D1. A larger density ratio seems to suppress the wrinkling of flame surface to some extent for the reference case. The cases U1 and U2 with lower turbulent intensities show less wrinkling and shorter flame brush thicknesses than the reference case. Although they have the same integral length scale, the characteristic scale of wrinkling shows apparent increase to give a reduced flame surface density at a lower turbulent intensity. Variation with respect to turbulent intensity, however, is not monotonic here, since the case U2 shows a higher peak than the case U1. The case S1 has a thicker laminar flamelet with a lower laminar flame speed than the other cases. The case S1 also has a thicker flame brush and a lower peak flame surface density than the reference case. The cases L1 and L2 have lower integral length scales with the turbulent intensity the same as the reference case. The flame brush thickness tends to decrease with a decreasing integral length scale, while the flame surface density does not show a monotonic behavior.

Flame surface densities for the six parametric cases show a similar trend as for the reference case in Fig. 6. The level of fluctuation varies with the maximum fluctuation for the case D1 and the minimum fluctuation for the case S1. It may be inferred that the fluctuation is partly related with accuracy of the estimation method based on the gradient of instantaneous reaction progress variable in the domain. The case S1 shows less fluctuation since it has a thicker laminar flamelet which allows more accurate estimation of the gradient. As for the reference case the turbulent burning velocity is predicted in

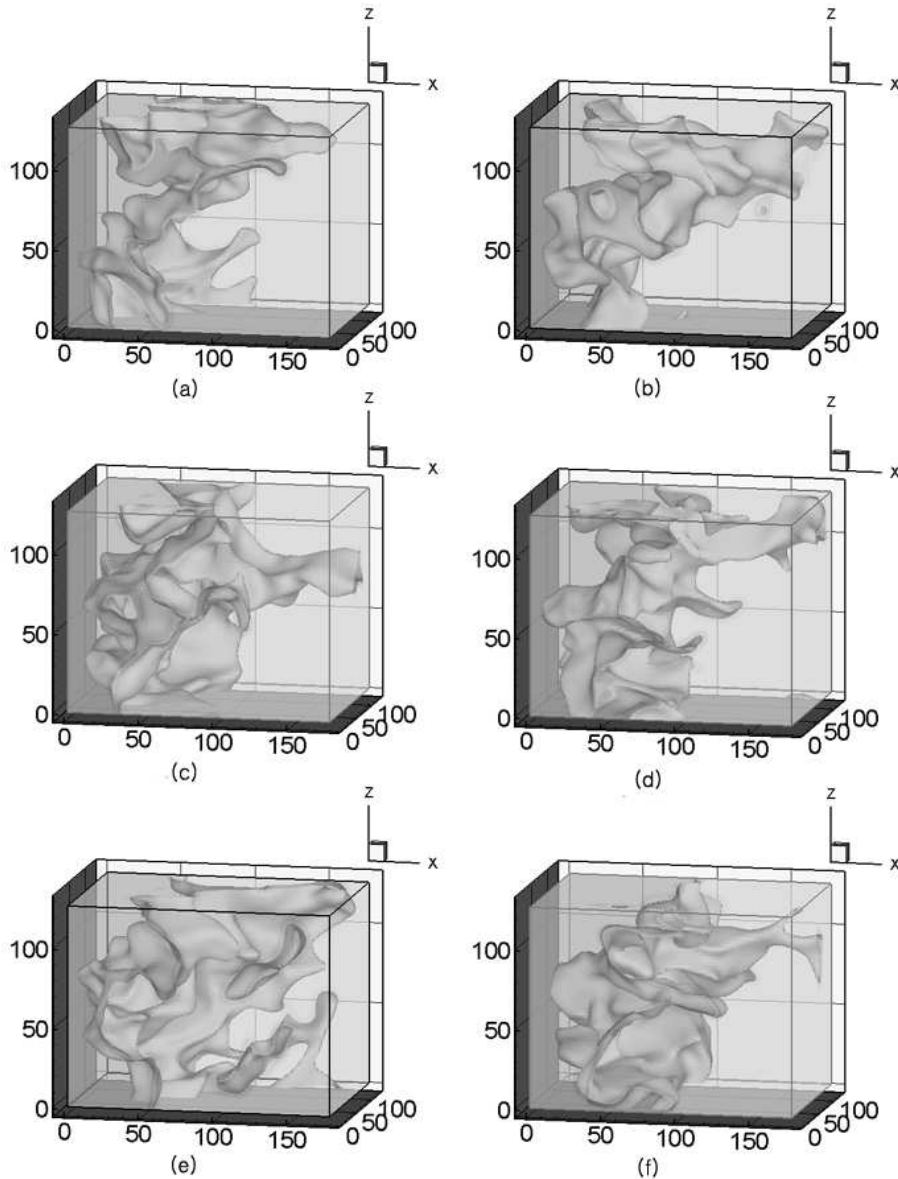


FIGURE 2. Images of a turbulent premixed flame brush at different instants for the reference case. (a) $5.0 \tau_t$, (b) $6.7 \tau_t$, (c) $8.3 \tau_t$, (d) $10.0 \tau_t$, (e) $11.7 \tau_t$ and (f) $13.4 \tau_t$.

terms of the maximum flame surface density on the upper boundary of the scattered points in Fig. 6. Without further study and more test cases in a larger domain it seems difficult to find a consistent trend for the maximum flame surface density and the level of fluctuation in terms of the independent parameters under investigation. Figure 7 shows instantaneous turbulent burning velocities with mean values given as horizontal lines for all cases. There is no obvious correlation between fluctuation in the predicted turbulent burning velocity in Fig. 7 and fluctuation of the flame surface density in Fig. 6.

Comparison is made between the mean turbulent burning velocities from DNS and the

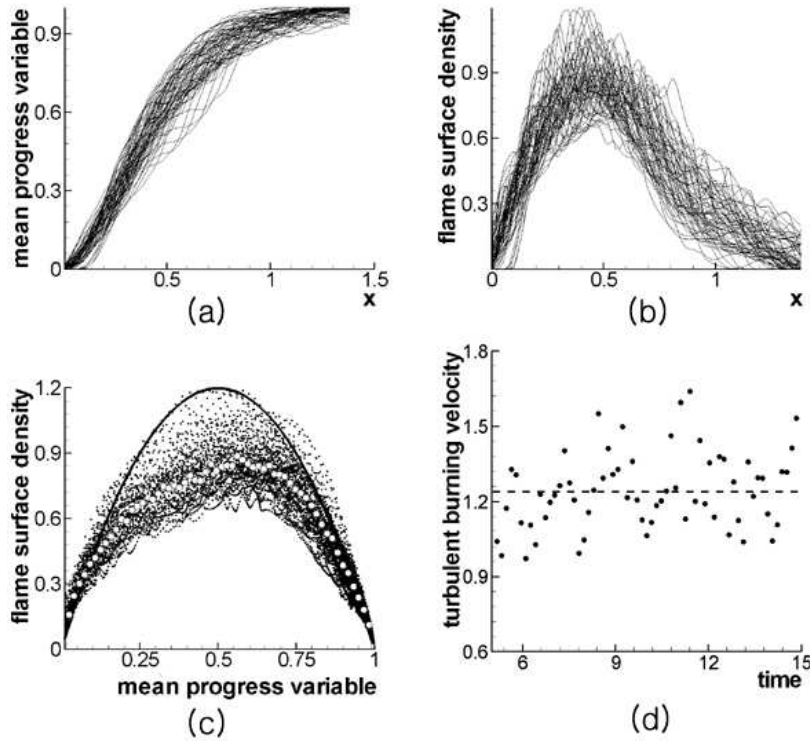


FIGURE 3. DNS results for the reference case.

predictions by Eq. (2.21). The maximum flame surface densities from the upper boundaries of scattered points are listed in Table 3. The function, $f(u'/S_{Lu}^0, Ka)$, and the mean stretch factor, I_0 , are assumed to be equal to unity. Although not a satisfactory practice, this simplifying assumption is not likely to affect overall validity of the comparison in this study. Turbulent diffusivity is estimated from $D_{tu} = u'^2 T_L$ where the Lagrangian integral time scale, T_L , has been estimated or measured in a few previous investigations in the literature. It is given in terms of the constant, C_0 , as $T_L^{-1} = \frac{3}{4} C_0 \frac{\varepsilon}{k}$. The constant, C_0 , was estimated to be about 2.1 from thermal wake data, while Pope (1994) reported a value in the range between 4 and 6. By fitting to direct simulation data Sawford (1991) suggested a value of 7, which is employed in the comparison in this report. All the relevant parameters are listed with the measured and estimated turbulent burning velocities in Table 3. There is good agreement between DNS and asymptotic expression in Fig. 8 where the points for all test cases are clustered around the line, $y=x$. The maximum error is about 15%.

5. Conclusions and future work

It is shown that the predictive formula for turbulent burning velocity agrees well with DNS results for a steady turbulent premixed flame in all test cases. There is no external pressure gradient to be taken into account in this one dimensional configuration. A parametric study was performed with respect to turbulent intensity, integral length scale, density ratio and laminar flame speed. Although some uncertainty remains for estimation of stretch factors and turbulent diffusivity, validity of the predictive formula is confirmed

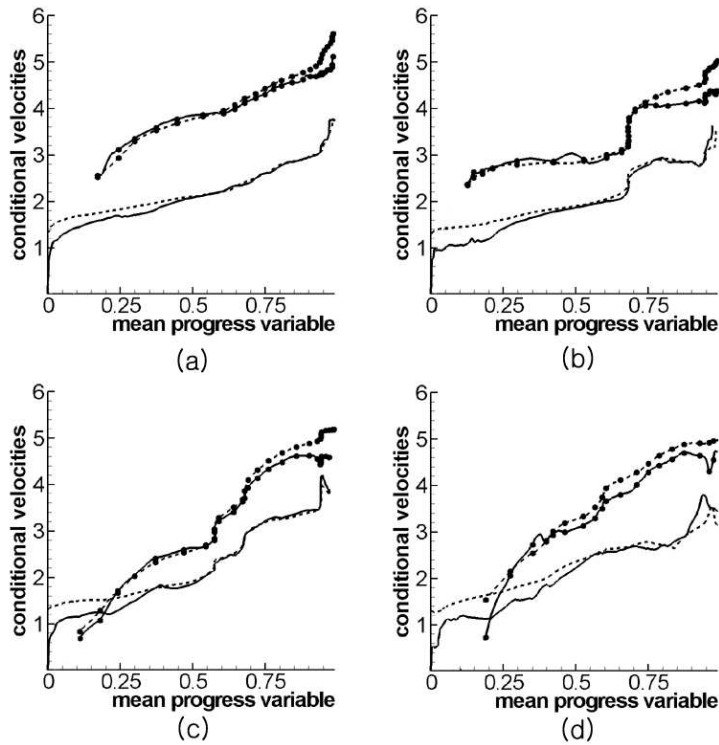


FIGURE 4. Conditional velocities at different instants for the reference case. Solid line for $\langle v \rangle_{su}$, dotted line for $\langle v \rangle_u$, solid line with markers for $\langle v \rangle_{sb}$ and dotted line with markers for $\langle v \rangle_b$.

Case Identification	Parameter Investigated
D1	$\rho_u/\rho_b = 1.0$
U1	$u' = 0.3736$
U2	$u' = 0.1868$
S1	$S_{Lu}^0 = 0.181$
L1	$l_t = 0.5841$
L2	$l_t = 0.3894$

TABLE 2. Six cases for parametric study

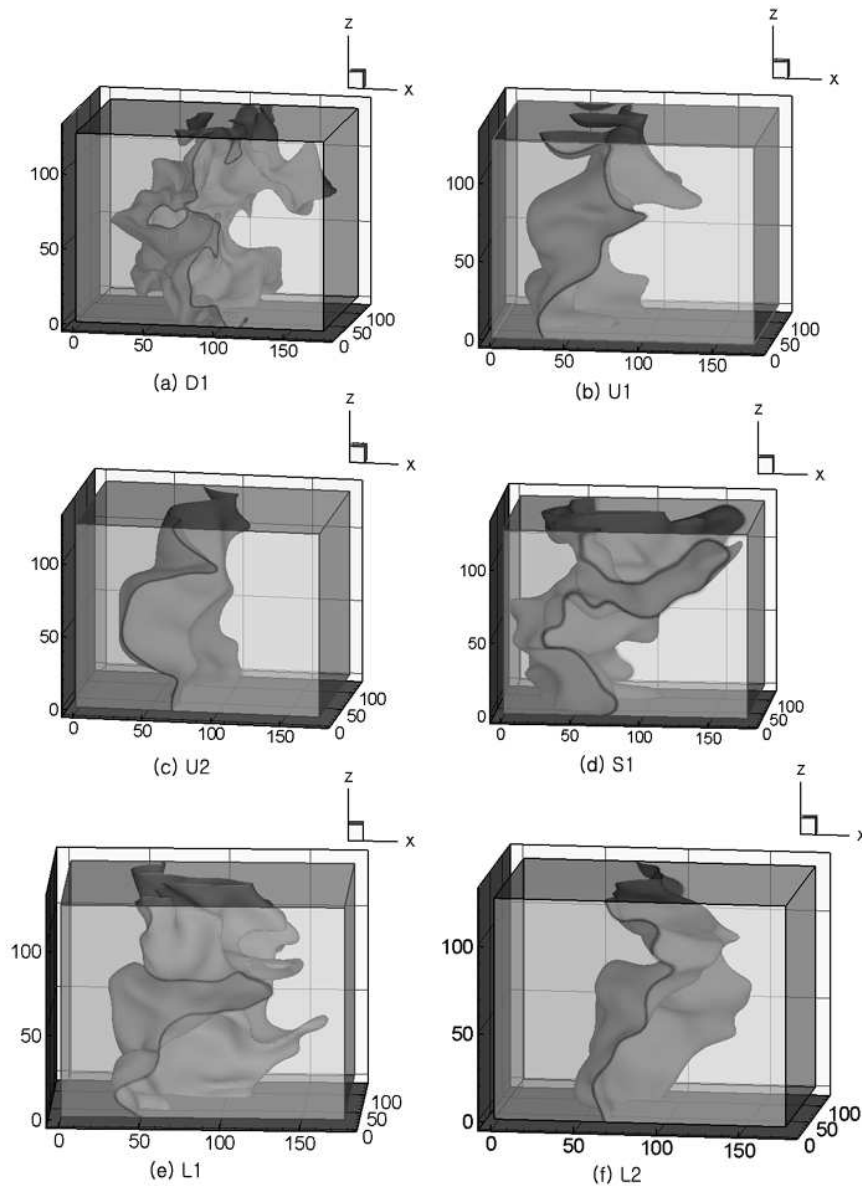


FIGURE 5. Images of turbulent premixed flame brushes for six parametric test cases.

in this investigation. DNS results show significant fluctuation of spatially averaged values on each cross sectional plane due to a limited computational domain and an insufficient number of samples for averaging. Correlation is made in terms of the maximum flame surface density on the upper boundary of scattered data points. Turbulent diffusivity is estimated from the Lagrangian integral time scale with the Kolmogorov constant, C_0 , equal to 7. Further work is needed to reduce fluctuation of statistical averages in a larger computational domain and to perform DNS of a more realistic flame with multistep

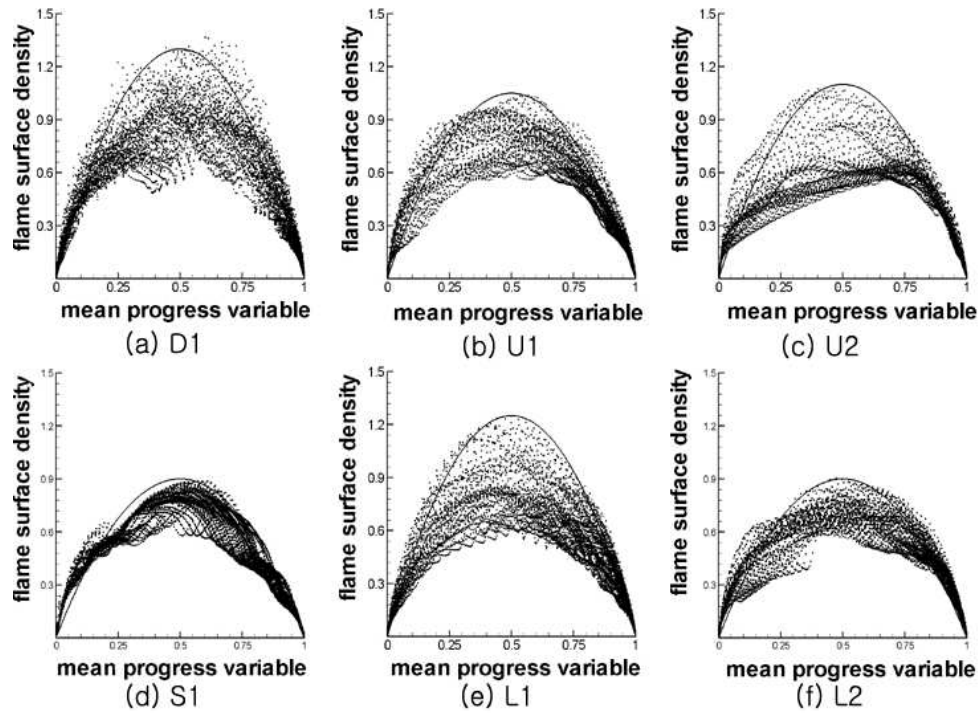
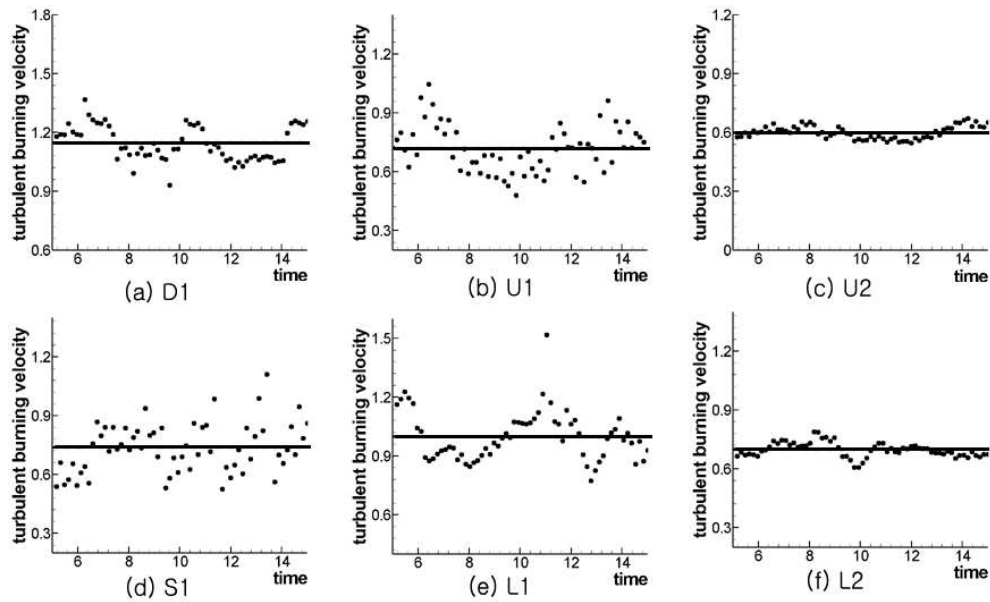
FIGURE 6. Flame surface density vs \bar{c} for six parametric test cases.

FIGURE 7. Turbulent burning velocities for six parametric test cases.

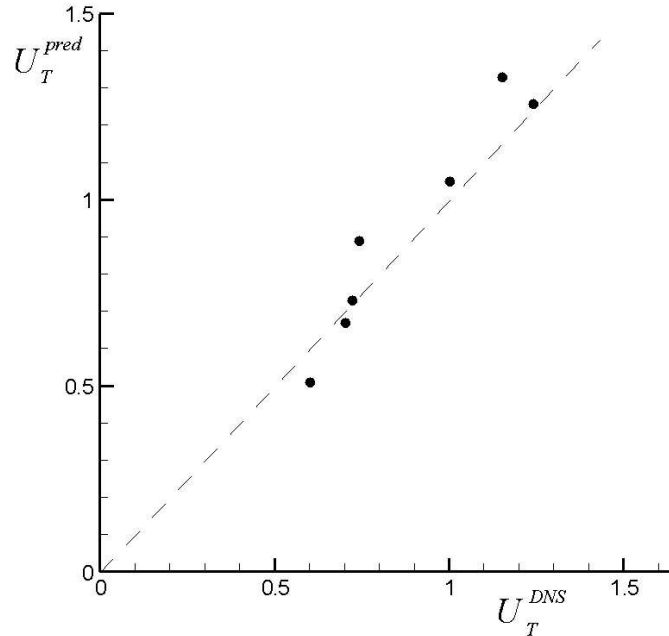
Case	D_{tu}	S_{Lu}^0	Σ_{max}	U_T^{DNS}	U_T^{pred}
ref	0.1961	0.314	1.21	1.24	1.26
D1	0.1916	0.314	1.30	1.15	1.33
U1	0.0981	0.314	1.05	0.72	0.73
U2	0.0438	0.314	1.10	0.6	0.51
S1	0.1961	0.181	0.90	0.74	0.89
L1	0.1471	0.314	1.25	1.00	1.05
L2	0.0981	0.314	0.90	0.70	0.67

TABLE 3. Comparison of turbulent burning velocity from DNS and predictive formula

chemistry and nonunity Lewis numbers. The effect of an external pressure gradient may easily be taken into account in the current steady one dimensional simulation.

REFERENCES

- ABDEL-GAYED, R. G., BRADLEY, D. & D. & LAWES, M. 1987 Turbulent burning velocities: A general correlation in terms of strain rates. *Proc. Roy. Soc. Lond.* **A414**, 389-413.
- DESCHAMPS, B., BOUKHALFA, A., CHAUVEAU, C., GOKALP, L., SHEPHERD, L. G. & CHENG, R. K. 2004 *An experimental estimation of flame surface density and mean reaction rate in turbulent premixed flames*. 24th Int. Symp. on Combustion (Combustion Institute), 469-475.
- DRISCOLL, J. F. 2003 *Premixed turbulent combustion - current knowledge and new challenges*. 3rd Joint Meeting of the U.S. Sections of the Combustion Institute, March, Chicago IL.
- IM, Y., HUH, K. Y., NISHIKI, S. & HASEGAWA, T. 2004 *Zone conditional assessment of flame-generated turbulence with DNS database of a turbulent premixed flame*. *Combustion & Flame* **137**, 478-488.
- KHOKHLOV, A. M, ORAN, E. S & WHEELER, J. C. 1996 *Scaling in buoyancy-driven turbulent premixed flames*. *Combustion & Flame* **105**, 28-34.
- KIM, S. H. & HUH, K. Y. 2004 *Second-order conditional moment closure modeling of turbulent piloted Jet diffusion flames*. *Combustion & Flame* in press.
- KLIMENKO, A. Y. & BILGER, R. W. 1999 *Conditional moment closure for turbulent combustion*. *Prog. Energy Combust. Sci.* **25**, 595-687.
- KOBAYASHI, H., TAMURA, T., MARUTA, K., NIIOKA, T. & WILLIAMS, F. A. 1996 *Burning velocity of turbulent premixed flames in a high pressure environment*. 26th Int. Symp. on Combustion (Combustion Institute), 389-396.

FIGURE 8. U_T^{DNS} vs U_T^{pred} .

- LEE, E. & HUH, K. Y. 2004 *Zone conditional modeling of premixed turbulent flames at a high Damkohler number*. *Combustion & Flame* **138**, 211-224.
- LEE, E., IM, Y. H. & HUH, K. Y. 2004 *Zone conditional analysis of a freely propagating one-dimensional turbulent premixed flame*. 30th Int. Symp. on Combustion (Combustion Institute) in press.
- LEE, G., HUH, K. Y. & KOBAYASHI, H. 2000 *Measurement and analysis of flame surface density for turbulent premixed combustion on a nozzle-type burner*. *Combustion & Flame* **122**, 43-57.
- LIU, L. & LENZE, B. 1988 *The influence of turbulence on the burning velocity of premixed CH₄-H₂ flames with different laminar burning velocities*. 22nd Int. Symp. on Combustion (Combustion Institute), 747-754.
- NISHIKI, S., HASEGAWA, T., BORGHI, R. & HIMENO, R. 2002 *Modeling of flame generated turbulence based on direct numerical simulation databases*. 29th Int. Symp. on Combustion (Combustion Institute), 2017-2022.
- PETERS, N. 1999 *The turbulent burning velocity for large scale and small scale turbulence*. *J. Fluid Mech.* **384**, 107-132.
- POPE, S. B. 1994 *Lagrangian PDF methods for turbulent flows.*, *Annu. Rev. Fluid Mech.* **26**, 23-63.
- SAWFORD, B. L. 1991 *Reynolds number effects in Lagrangian stochastic models of turbulent dispersion.*, *Phys Fluids A* **3**(6), 1577-1586.